



Received on 26 November, 2015; received in revised form, 23 February, 2016; accepted, 23 March, 2016; published 01 May, 2016

POLY (METH) ACRYLATES NANOSPHERES OF CENTRALLY ACTING ANALGESIC DRUG FOR POSTOPERATIVE PAIN: *IN-VITRO* AND *IN-VIVO* CHARACTERIZATION STUDY

Sukhbir Singh ^{*1,2}, Neelam Sharma ², Yash Paul Singla ³ Sandeep Arora ² and Jitender Madan ⁴

Department of Research¹, Innovation and Consultancy, Punjab Technical University, Jalandhar-Kapurthala Highway, Kapurthala - 144603, Punjab, India.

Chitkara College of Pharmacy ², Chitkara University, Chandigarh Patiala National Highway (NH-64), Patiala - 140401, Punjab, India.

Lord Shiva College of Pharmacy ³, Sirsa - 125055, Haryana, India.

Chandigarh College of Pharmacy ⁴, Landran, Kharar, Sahibzada Ajit Singh Nagar, 140307 Punjab, India

Key words:

Postoperative pain,
Dissolution efficiency, Fickian
diffusion, Mechanical allodynia

Correspondence to Author:

Sukhbir Singh,

Assistant Professor
Chitkara College of Pharmacy,
Chitkara University, Chandigarh
Patiala National Highway (NH-64),
Patiala-140401, India.

E-mail: singh.sukhbir12@gmail.com

ABSTRACT: Postoperative pain management is prerequisite element for care of surgical patient. Objective of this study was to develop and evaluate nefopam hydrochloride loaded poly (meth) acrylates nanospheres (NFH-NS) for post-incisional pain treatment. Nefopam hydrochloride (NFH) is a centrally acting, non-opioid analgesic exclusive for treatment of post-incisional pain. NFH-NS were fabricated using eudragit RL 100: RS 100 by quasi solvent diffusion technique to provide sustained release of NFH. Entrapment efficiency (% EE), drug loading (% DL), z-average, polydispersity index and zeta potential (ζ) of NFH-NS was found $84.972 \pm 1.23\%$, $21.41 \pm 2.02\%$, 648 ± 4.8 nm, 0.53 and + 4.48 mV, respectively. Scanning electron micrographs asserted smooth morphology and substantial spherical shape of nanospheres. In-vitro dissolution test revealed that NFH-NS followed fickian diffusion for drug transport. Mean dissolution time, dissolution efficiency and difference factor (f1) for NFH-NS was 5.68 h, 68.9 % and 31.83, respectively, which indicated dissimilarity in dissolution profiles as compared to NFH. % EE and % DL of NFH-NS at $25 \pm 2^\circ\text{C}/60 \pm 5\%$ RH and $40 \pm 2^\circ\text{C}/75 \pm 5\%$ RH revealed stability of formulation. Maximum % reversal of mechanical allodynia was achieved after peroral administration of NFH-NS (30 mg kg⁻¹) in rat model of post-incisional pain for 14 days. Minimum effective dose (MED) and ED50 of NFH-NS was found 10 mg kg⁻¹ and 16.4 mg kg⁻¹, respectively.

INTRODUCTION: Drug delivery is multifaceted and autonomous field of research ¹. Polymeric drug delivery systems have been extensively employed to provide captivating substitute for dynamic and long-term delivery of therapeutic agents. Polymeric dosage forms contribute many benefits such as reduced frequency of drug administration, site-specific and sustained delivery of drugs ²⁻⁴.

Polymeric nanosphere delivery systems have proficiency to enhance drug stability, upgrade its duration of therapeutic effect and diminish its degradation as well as metabolism ⁵⁻⁸.

Postoperative pain management is prerequisite element for care of surgical patient. Most of patients suffer from severe pain during the first few days post-surgery ^{9, 10}. Therefore, post-incisional pain has great significance for investigation ^{11, 12}. Nefopam hydrochloride (NFH) is a non-opioid analgesic that acts centrally by inhibiting reuptake of triple neurotransmitter *i.e.* dopamine (DA), noradrenalin (NA) and 5-hydroxytryptamine (5-HT) to maintain adequate monoamines in presynaptic cleft ^{11, 13}. Other mode of action may be

QUICK RESPONSE CODE 	DOI: 10.13040/IJPSR.0975-8232.7(5).1967-77
	Article can be accessed online on: www.ijpsr.com
DOI link: http://dx.doi.org/10.13040/IJPSR.0975-8232.7(5).1967-77	

through blockage of NMDA mediated glutamatergic transmission of calcium influx or voltage-gated sodium channels which leads to anti-nociceptive effect¹⁴⁻¹⁶. It has been reported in literature that plasma half-life, protein binding and oral bioavailability of NFH is 3-5 h, 75 % and 40 %, respectively¹⁴. NFH undergoes substantial hepatic biotransformation to desmethylnefopam (which seems to be biologically active) and N-oxide-nefopam¹⁷. Major route of elimination (87 %) is renal although a small part (8 %) is excreted in faeces¹⁸. Nefopam 20 mg was equipotent to morphine 6-12 mg or to meperidine 50 mg^{11, 19}. NFH is contemplated to be safe and well tolerated because it's reported adverse effects such as drowsiness, nausea, vomiting and sweating are minor^{9, 20, 21}. NFH neither affects platelet function like NSAIDS nor leads to addiction or tolerance like opioid. It has been exclusive drug for treatment of post-incisional and neuropathic pain. It can be used for relief of dental, musculo-skeletal, acute traumatic, acute wound and cancer pain^{18, 22-24}.

Objective of this research was to develop and evaluate nefopam hydrochloride loaded poly (meth) acrylates nanospheres (NFH-NS) for post-incisional pain management. In this study, NFH-NS were fabricated using eudragit RL 100: RS 100 by quasi solvent diffusion technique to provide sustained release of NFH and characterized for various parameters such as entrapment efficiency, drug loading, mean particle size, polydispersity index, zeta potential and scanning electron micrographs. *In-vitro* drug release characteristics and stability studies were also investigated. In addition, potency and efficacy of NFH-NS was investigated in a rat model of post-incisional pain.

MATERIAL AND METHODS:

Materials:

Nefopam hydrochloride (C₁₇H₂₀ClNO, 5-methyl-1-phenyl-1, 3, 4, 6-tetrahydro-2, 5-benzoxazocine hydrochloride, Mw 289.8 g mol⁻¹, CAS NO-23327-57-3, 99.57% purity) was procured from Hangz Hou-Daying-Chem. Company Ltd. China. Eudragit RL 100 and RS 100 were received as gift sample supplied by Evonik Industries AG, Mumbai, India. Span 80 (sorbitan monooleate, HLB-4.3), magnesium stearate (magnesium octadecanoate, 591.27 g mol⁻¹), sodium hydroxide, potassium

dihydrogen phosphate and methanol were obtained from Loba Chemicals Private Limited, Mumbai, India. Acetone (2-propanone, C₃H₆O, Mw 58.08 g mol⁻¹), heavy liquid paraffin and n-hexane (C₆H₁₄, Mw 86.18) were obtained from Merck Specialties Private Limited, Mumbai. Petroleum ether was purchased from Thomas Bakers Chemical Private Limited, Mumbai. Isoflurane was procured from Sigma, USA. All other chemicals utilized were of analytical grade.

Animals:

Animal experiments were carried out with prior permission from institutional animal ethics committee (IAEC/CCP/13/PR-010) and care of the animals was carried out as per the guidelines of committee for the purpose of control and supervision of experiments on animals (CPCSEA), ministry of environment and forest, government of India (Chitkara college of pharmacy animal facility registration number: 1181/ab/08/CPCSEA). Rats (male wistar, 180-200 g) were used in all experiments and allowed free access to food and water. All the animals were maintained on 12 h light-dark cycle in temperature and humidity controlled rooms. Efforts were made to restraint affliction and to utilize minimum number of animals essential to achieve statistical significance.

Preparation of poly (meth) acrylates nanospheres:

Quasi solvent diffusion technique was successfully employed for fabrication of nefopam hydrochloride-loaded poly (meth) acrylates nanospheres (NFH-NS) which were composed of 1: 3 molar ratios of NFH and poly (meth) acrylates (eudragit RL 100: RS 100; 1: 2). Accurate quantity of NFH, eudragit RL 100 and RS 100 were dissolved in acetone-ethanol solvent mixture to form dispersed phase (DP). Continuous phase (CP) consist of heavy liquid paraffin containing n-hexane as hardening agent and sorbitan monooleate as an emulsifier. DP was extruded slowly through syringe # 20 to CP to form dispersion. After continuous stirring for 4 h on magnetic stirrer (Remi Instruments Division, India) at 38 ± 0.5°, dispersion was centrifuged and washed with petroleum ether. Nanospheres were accumulated by filtration utilizing 0.22 µm membrane filters followed by ultracentrifugation at 20,000 rpm for

30 minutes applying cooling centrifuge (RIS-24 BL, Remi Instruments Division, and India) and freeze-dried using lyophilizer (ISIC Make, India). Schematic representation for fabrication of NFH-NS is delineated in Fig. 1.

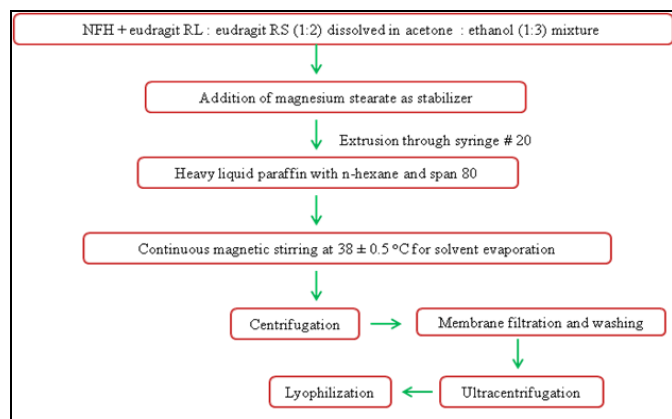


FIG. 1: SCHEMATIC REPRESENTATION OF EXPERIMENTAL PROCEDURE FOR FABRICATION OF NFH-NS

Characterization of NFH-NS:

Entrapment efficiency and drug loading determination:

50 mg of NFH-NS was accurately weighed and extracted with phosphate buffer, pH 7.4 for 24 h and centrifuged for 10 min at 3500 rpm. Supernatant was withdrawn and analyzed spectrophotometrically at 266 nm (Systronics AU2701). NFH concentration in the sample was determined using calibration curve regression equation. Entrapment efficiency (% EE, w/w) and drug loading (% DL, w/w) of NFH-NS was calculated by following equations^{25, 26}:

$$\% \text{ EE, w/w} = \frac{\text{Weight of drug entrapped}}{\text{Weight of drug}} \times 100 \quad \text{Eq. (1)}$$

$$\% \text{ DL, w/w} = \frac{\text{Weight of drug entrapped}}{\text{Weight of drug} + \text{Weight of polymer}} \times 100 \quad \text{Eq. (2)}$$

Particle size distribution by dynamic light scattering (DLS):

Z-average and polydispersity index (PDI) of NFH-NS was determined by dynamic light scattering (DLS) using zetasizer ver. 7.03 (Nano ZS, Malvern Instruments Ltd., UK). Analysis was performed at 25°C using disposable size cuvette at count rate of 165.6 kcps. Double distilled water with refractive index and viscosity of 1.330 and 0.8872 cP,

respectively, was utilized for dilution of sample (500 ×).

Zeta potential (ζ) analysis:

NFH-NS was characterized by zeta potential (ζ) analysis using zetasizer ver. 7.03 (Nano ZS, Malvern Instruments Ltd., UK). Double distilled water with refractive index, dielectric constant and viscosity values 1.330, 78.5 and 0.8872, respectively, was used for diluting sample to appropriate concentration. Sample was placed in clear disposable zeta cell and analyzed at count rate of 29.3 kcps.

Surface morphology of nanospheres:

Surface morphology of NFH-NS was investigated using scanning electron microscopy (SEM). Nanospheres were coated with gold palladium for 150 seconds to apply 20 nm films under an atmosphere of air (Coater Polaron, 18mA current at 1.4 kV) and examined with a variable pressure scanning electron microscope (Hitachi S3400N).

In-vitro dissolution test:

In-vitro drug release profile study:

Dialysis bag diffusion technique was used for *in-vitro* drug release profile study of NFH-NS^{27, 28}. Diffusion membrane with molecular weight cut-off (MWCO) of 12,000-14,000 Da (Himedia, India) was soaked in phosphate buffer, pH 7.4 for 12 h before being used for experiment²⁹. NFH or NFH-NS was placed in dialysis bag which was sealed at both ends. Dialysis bag was immersed in 50 mL of phosphate buffer, pH 7.4, which was stirred at 200 rpm on magnetic stirrer (Remi, India) and maintained at 37 ± 0.5 °C. Two mL sample was withdrawn at regular time intervals (0.5, 1, 2, 4, 6, 8, 12, 16, 24 h) and reloaded with equivalent volume of fresh release medium.

Concentration of NFH in sample was analyzed by UV spectrophotometry at 266 nm using double beam UV spectrophotometer (Systronics AU2701, India). All the experiments were performed in triplicate ($n = 3$), and the average values were taken. Cumulative drug released (%) vs. time (h) were plotted to observe *in-vitro* drug release pattern from NFH-NS and free NFH^{6, 30}.

In-vitro drug release kinetics analysis by mathematical-models:

In order to investigate the release mechanism of drug from NFH-NS, *in-vitro* drug release data was analyzed using various mathematical models *i.e.* zero-order kinetics, first-order kinetics, Hixson-crowell cube root model, Higuchi model, Korsmeyer-peppas model, and Weibull model employing Eqs. (3) - (8), respectively. Plotted data were fitted with linear regression to obtain regression equation and coefficient (r^2)^{31,32}.

$$F = K_0 t \quad \text{Eq. (3)}$$

$$\ln(1 - F) = K_f t \quad \text{Eq. (4)}$$

$$1 - \sqrt[3]{1 - F} = k_{1/3} t \quad \text{Eq. (5)}$$

$$F = K_H \sqrt{t} \quad \text{Eq. (6)}$$

$$\ln F = \ln K_p + p \ln t \quad \text{Eq. (7)}$$

$$\ln[-\ln(1 - F)] = \beta \ln t_d + \beta \ln t \quad \text{Eq. (8)}$$

Where, F denotes fraction of drug released up to time t ; K_0 , K_f , K_H , p , K_p , $K_{1/3}$, t_d and β are parameters of models.

Comparison of in-vitro drug release profile by model-independent methods:

Model independent methods *i.e.* ratio test and pair-wise procedure were used for comparison of *in-vitro* drug release profiles of NFH and NFH-NS. For ratio test, comparison was made on basis of mean dissolution time (MDT) calculated using following equation:

$$\text{MDT} = \frac{\sum_{j=1}^n t_j \Delta M_j}{\sum_{j=1}^n \Delta M_j} \quad \text{Eq. (9)}$$

Where, j is sample number; n is number of dissolution sample times; t_j and ΔM_j are time at midpoint and additional amount of drug dissolved between t_j and t_{j-1} , respectively.

For pair-wise comparison, difference factor (f_1) which measured percent error between *in-vitro* drug release curves of NFH and NFH-NS over all time intervals was calculated using Eq. (10). Dissolution efficiency (% DE) used to characterize

drug release profile was calculated applying Eq. (11) and (12)^{31,33,34}.

$$f_1 = \frac{\sum_{j=1}^n |R_j - T_j|}{\sum_{j=1}^n |R_j|} \times 100 \quad \text{Eq. (10)}$$

$$\% \text{ D.E.} = \frac{SA}{R} \times 100 \quad \text{Eq. (11)}$$

$$\% \text{ D.E.} = \frac{\int_0^t y \times dt}{y_{100} \times t} \times 100 \quad \text{Eq. (12)}$$

Where, n is sampling number; R and T is percent dissolved of NFH and NFH-NS at each time point j ; SA = Shaded area under *in-vitro* drug release curve up to time t ; R = Rectangle area ($y_{100} \times t$) described by 100% dissolution up to time t and y is drug percent dissolved at time t .

Stability study:

Following ICH guidelines Q1A (R2), NFH-NS were kept in sealed glass vials at elevated temperatures and relative humidity in stability analysis test chamber (CHM 10S, REMI, India) at $25 \pm 2^\circ\text{C}/60 \pm 5\% \text{ RH}$ and $40 \pm 2^\circ\text{C}/75 \pm 5\% \text{ RH}$ over a period of 12 months for conducting long term and accelerated stability testing, respectively^{35, 36}. Samples were withdrawn at preset time intervals of 3, 6 and 12 months and characterized for change in % EE and % DL (as per aforementioned protocol).

In-vivo evaluation:

Drug administration:

NFH and NFH-NS were dissolved in phosphate-buffer solution. Isoflurane was used for anesthesia in incisional pain model. Animals were randomly divided into several experimental groups: 1 - phosphate-buffer solution (5 ml kg^{-1}) treated control group, 2 - NFH (10 mg kg^{-1}) treated reference group, 3 - NFH-NS (10 mg kg^{-1}) treated test group-I, 4 - NFH-NS (20 mg kg^{-1}) treated test group-II, and 5 - NFH-NS (30 mg kg^{-1}) treated test group-III. Sham group was included in incisional pain model. All drug preparations were administered by peroral (p.o) route using oral gavage.

Post-incisional pain study by incisional pain model:

Surgery: Surgery of rats was conducted after anaesthetization with 2% isoflurane. Using sterile technique, 1 cm longitudinal incision was made with 10 # scalpel, through skin and fascia of plantar aspect of left hind paw, starting 0.5 cm from proximal edge of heel and extending toward toes. Skin was opposed with two single interrupted sutures using 5-0 nylon with gentle pressure. Povidone-iodine antibiotic powder (Cipladine, Cipla Ltd. Mumbai, India) was sprinkled over wound site and animals were allowed to recover in their home cages^{10, 12, 37}. Sham-operated rats received anesthesia, but not an incision.

Treatment of injury:

Von Frey paw withdrawal threshold (VFWT) was determined prior to surgery (baseline) on day 0 and 24 h post-ligation (pre-dose) on day 1, for each rat of different groups. Drug preparations were administered immediately after the pre-dose test and continued daily to day 14 post-ligation. Behavioral test (mechanical allodynia) was recorded at different time intervals (0.5, 1, 2, 4, 6, 8, 10 h, 3, 5, 7 and 14 day) post-dose treatment.

Behavioral test (mechanical allodynia):

Automated electronic von Frey nylon monofilaments (Stoelting, USA) were used to determine VFWT to non-noxious mechanical stimulus. Each rat was positioned on wire mesh cage with an uplifted metal screen surface. Electronic von Frey employed a single nonflexible filament to which experimenter implemented an increasing force. Stimulus was applied progressively to plantar surface of left hind paw of individual animal. End point was contemplated as nocifensive paw withdrawal³⁸. Percent reversal of allodynia was determined using following equation:

$$\% \text{ reversal of allodynia} = \frac{\text{Postdose threshold} - \text{Predose threshold}}{\text{Baseline threshold} - \text{Predose threshold}} \times 100 \quad \text{Eq. (14)}$$

Statistical Analysis:

All the results were represented as mean value \pm standard deviation. Two-way ANOVA followed by bonferroni post-test for comparison and significance study was performed using GraphPad

Prism version 5.01 for windows (GraphPad Software, San Diego California, USA). Statistical difference ($p < 0.05$) was considered significant. Dose that produced 50% of the maximum percent reversal (ED_{50}) was calculated using the curve-fitting functions in GraphPad Prism 5.01.

RESULT AND DISCUSSION:

Characterization of NFH-NS:

Entrapment efficiency and drug loading of NFH-NS was $84.972 \pm 1.23\%$ and $21.41 \pm 2.02\%$, respectively. Entrapment and loading capacity of fabricated nanospheres was found satisfactorily high. Z-average and polydispersity index of nanospheres was found 648 ± 4.8 nm and 0.53, respectively (**Fig. 2**). Data illustrated homogeneity with comparatively narrow particle size distribution in nanometric range. Zeta potential (ζ) value of NFH-NS was determined + 4.48 mV (**Fig. 3**). Positive value of zeta potential may be attributed to cationic poly (meth) acrylates with quaternary ammonium group. Scanning electron micrographs asserted that nanospheres were substantially spherical in shape with smooth morphology (**Fig. 4**).

Statistical Analysis:

All the results were represented as mean value \pm standard deviation. Two-way ANOVA followed by bonferroni post-test for comparison and significance study was performed using GraphPad Prism version 5.01 for windows (GraphPad Software, San Diego California, USA). Statistical difference ($p < 0.05$) was considered significant. Dose that produced 50% of the maximum percent reversal (ED_{50}) was calculated using the curve-fitting functions in GraphPad Prism 5.01.

RESULT AND DISCUSSION:

Characterization of NFH-NS:

Entrapment efficiency and drug loading of NFH-NS was $84.972 \pm 1.23\%$ and $21.41 \pm 2.02\%$, respectively. Entrapment and loading capacity of fabricated nanospheres was found satisfactorily high. Z-average and polydispersity index of nanospheres was found 648 ± 4.8 nm and 0.53, respectively (**Fig. 2**). Data illustrated homogeneity with comparatively narrow particle size distribution in nanometric range. Zeta potential (ζ) value of NFH-NS was determined + 4.48 mV (**Fig. 3**).

Positive value of zeta potential may be attributed to cationic poly (meth) acrylates with quaternary ammonium group. Scanning electron micrographs asserted that nanospheres were substantially

spherical in shape with smooth morphology (Fig. 4).

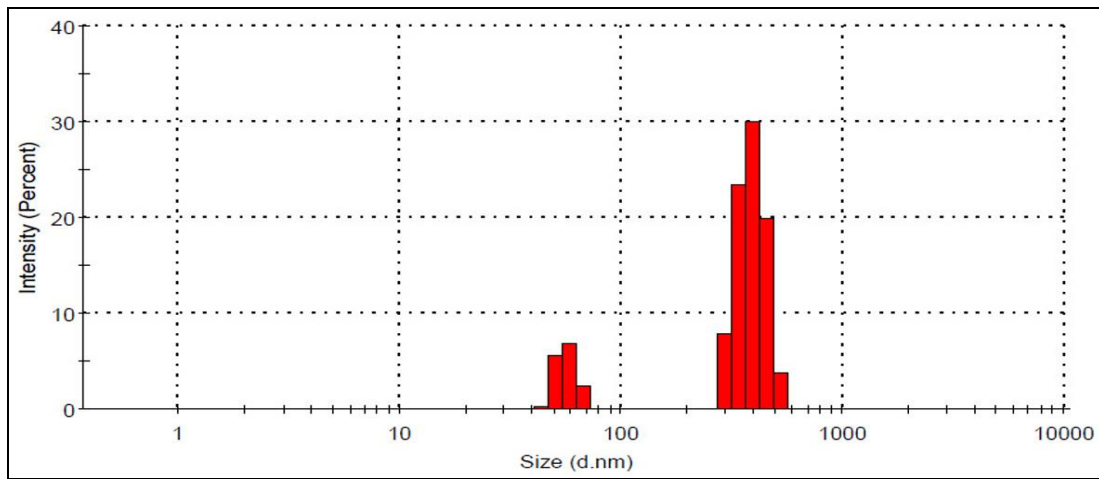


FIG. 2: PARTICLE SIZE DISTRIBUTION PATTERNS OF NFH-NS

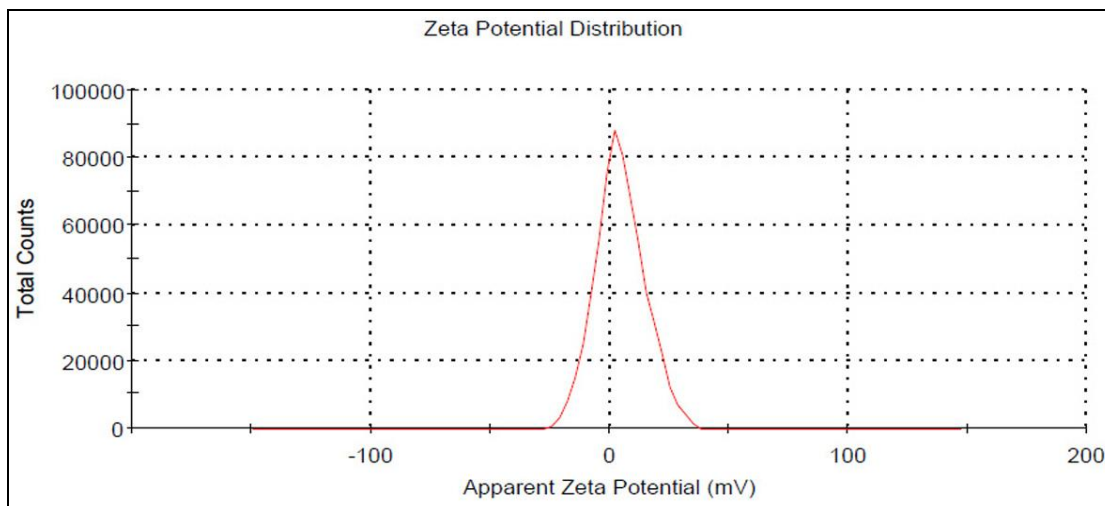


FIG. 3: APPARENT ZETA POTENTIAL REPORT OF NFH-NS

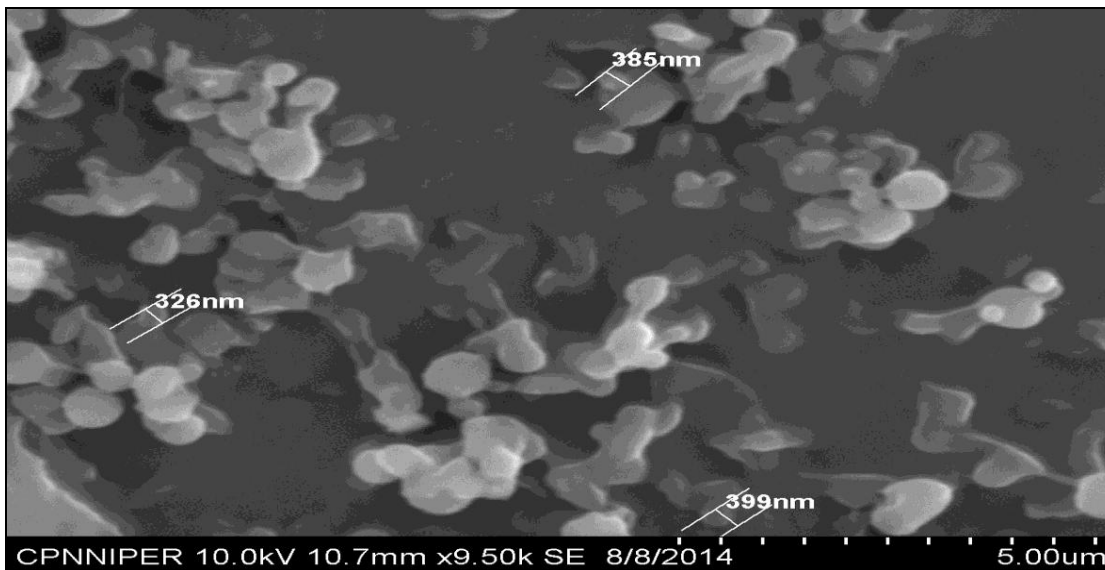


FIG. 4: SCANNING ELECTRON MICROGRAPHS OF NFH-NS AT (× 9500) MAGNIFICATION

In-vitro dissolution study:

NFH was released from NFH-NS following biphasic pattern with an initial ‘burst release’ of loosely bound NFH on or near the surface of particles during first 4 h and then sustained release of remaining drug from core due to diffusion from polymer matrix over 24 h. However, NFH rendered a rapid release of drug within 6 h (Fig. 5). Mechanism of drug release from NFH-NS was

resolved by finding R^2 value for various mathematical kinetic models viz. zero-order kinetics, first-order kinetics, Hixon-crowell, higuchi, korsmeyer-peppas and weibull model (Fig. 6). In-vitro drug release of NFH-NS was best explained by korsmeyer-peppas equation with regression coefficient (r^2), 0.988 (Fig. 6e). This indicated that NFH-NS followed fickian diffusion drug transport mechanism³¹.

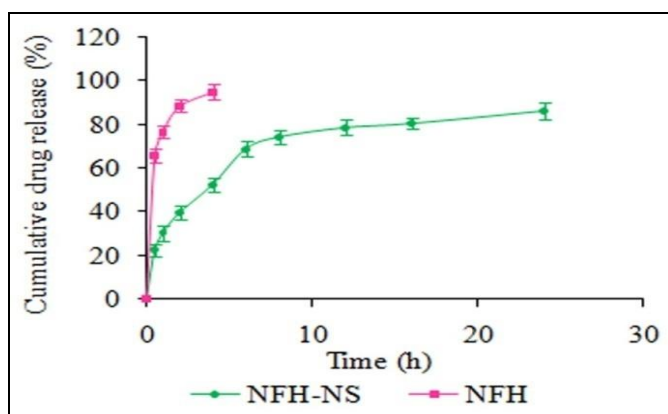


FIG. 5: IN-VITRO DRUG RELEASE PROFILES FROM NFH-NS AND NFH IN PHOSPHATE BUFFER, PH 7.4 AT 37 ± 0.5°C

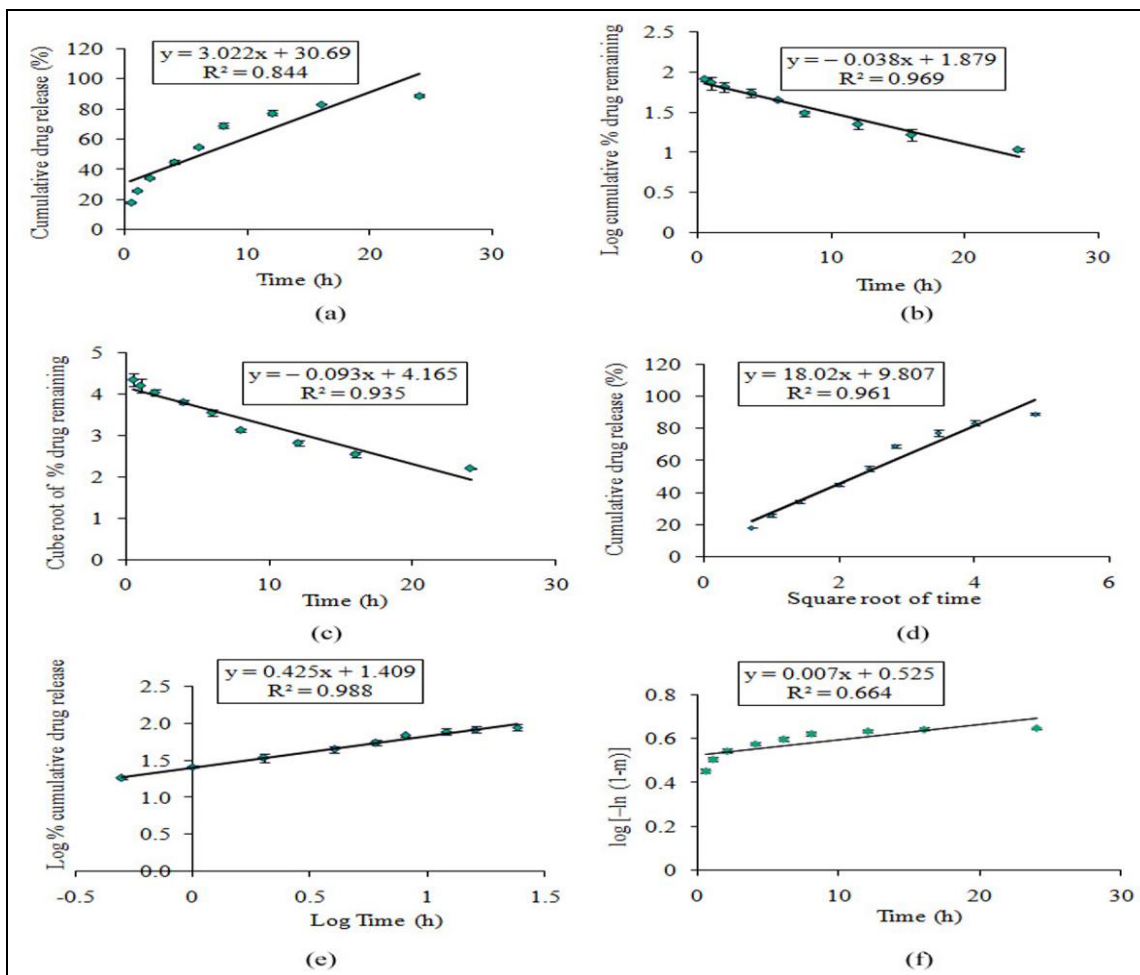


FIG. 6: IN-VITRO DRUG RELEASE KINETIC MODEL FOR NFH-NS (A) ZERO-ORDER, (B) FIRST-ORDER, (C) HIXON-CROWELL MODEL, (D) HIGUCHI MODEL, (E) KORSMEYER-PEPPAS MODEL, AND (F) WEIBULL MODEL

MDT for pure NFH and NFH-NS was found to be 2.12 and 5.68 h, respectively, (Table 1) which indicated that *in-vitro* drug release from nanospheres was considerably slower than from pure drug. Reason behind this might be entrapment of drug in poly (meth) acrylates polymers which gets swell in presence of water and digestive fluids and exhibit slow release by diffusion. % DE for NFH and NFH-NS was found 18.95 and 68.9 %, respectively (Table 1). Higher dissolution efficiency of NFH-NS could be due to increased surface area to volume ratio. In order to consider similar dissolution profiles between reference and test formulation, f_1 values should be lower than 15 (0-15). Difference factor (f_2) between NFH-NS and NFH was 31.83 which indicated dissimilarity between dissolution profiles as the value was > 15 ³¹.

TABLE 1: DISSOLUTION EFFICIENCY (% DE) AND MEAN DISSOLUTION TIME (MDT) OF NFH AND NFH-NS

Formulation	% DE	MDT
NFH	18.95	2.12
NFH-NS	68.90	5.68

Stability study:

Long term and accelerated stability testing of NFH-NS was conducted as per ICH guidelines Q1A (R2) and ICH Q1. NFH-NS were characterized for change in % EE and DL at predetermined time intervals of 3, 6 and 12 months. It was observed that there was no significant change ($p > 0.05$) in % EE and DL of samples kept at $40 \pm 2^\circ\text{C}/75 \pm 5\%$ RH as compared to those placed at $25 \pm 2^\circ\text{C}/60 \pm 5\%$ RH (Fig. 7) which revealed stability of formulation on storage at elevated temperature and humidity conditions.

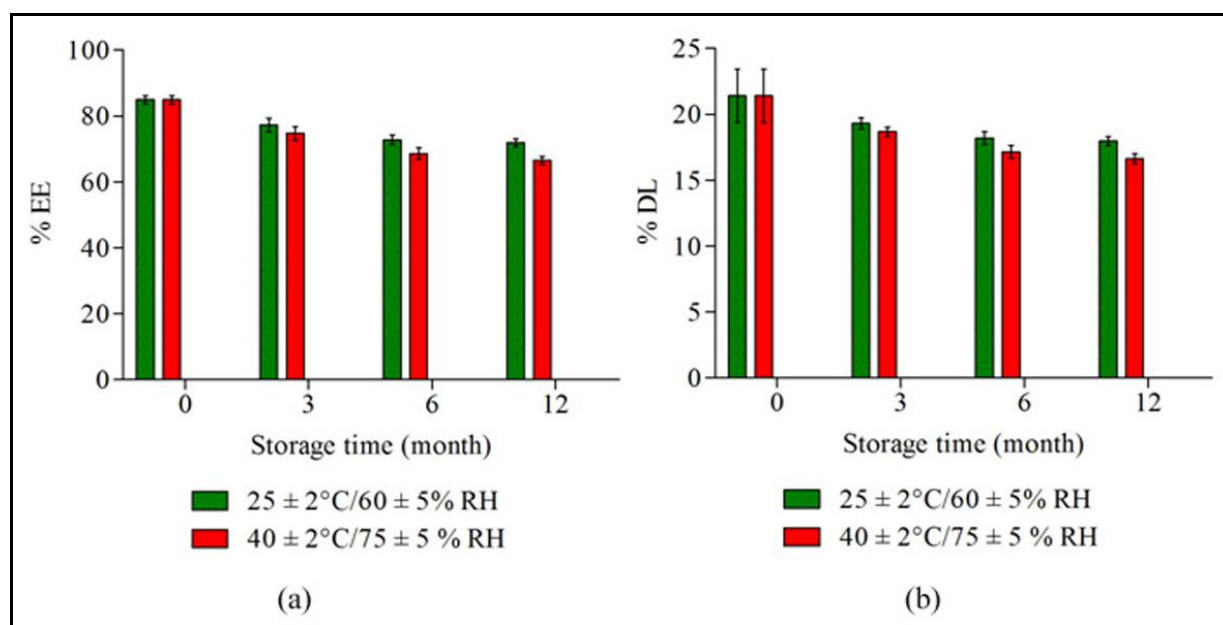


FIG. 7: % EE AND % DL OF NFH-NS AGAINST STORAGE TIME AT $25 \pm 2^\circ\text{C}/60 \pm 5\%$ RH AND $40 \pm 2^\circ\text{C}/75 \pm 5\%$ RH 25°C

In-vivo evaluation:

Postoperative pain study was performed by incisional pain model to compare NFH (10 mg kg^{-1}) and NFH-NS ($10\text{-}30 \text{ mg kg}^{-1}$) employing mechanical allodynia for behavioral testing of rats. VFWT determined by electronic von Frey assay prior to incision was 75.1 ± 2.4 (baseline). All rats underwent VFWT testing before treatment (pre-dose) followed by post-dose testing. Control group exhibited strong allodynia during experimental period as compared to NFH-NS treated groups ($p < 0.001$). On the contrary, phosphate-buffer treated sham group did not display mechanical allodynia

during experimental period. NFH-NS $10\text{-}30 \text{ mg kg}^{-1}$ treated group produced significant difference in VFWT till 14 day of drug administration as compared to NFH 10 mg kg^{-1} treated reference group ($p < 0.05$, $p < 0.01$, $p < 0.001$) (Fig. 8). Data illustrated sustained release of drug from NFH-NS. Furthermore, it was investigated that NFH-NS $20\text{-}30 \text{ mg kg}^{-1}$ treated animals exhibited significantly higher VFWT as compared to NFH-NS 10 mg kg^{-1} treated animals ($p < 0.001$, at all time points) which manifested that NFH-NS produced dose-dependent attenuation of pain.

Minimum effective dose (MED), onset and duration of action for NFH-NS was retrieved from the curve obtained in incisional pain model (**Fig. 8**). MED, minimum dose that elicited statistically significant response as compared to vehicle-treated controls was 10 mg kg^{-1} . Onset of action, earliest

detected statistically significant response with MED was found 0.5 h. NFH-NS exhibited long duration of action as indicated by statistically significant VFWT at various time points post-dose at MED (10 mg kg^{-1}) (**Fig. 8, Table 2**).

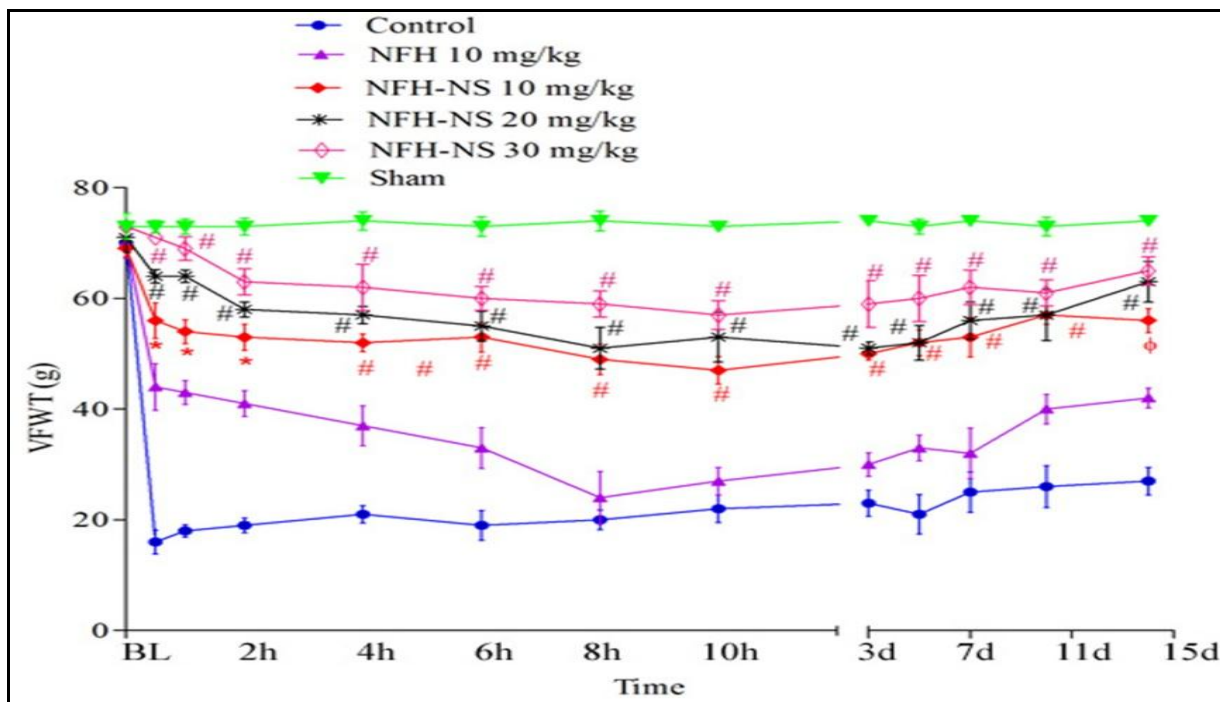


FIG. 8: VFWT FROM VARYING DOSES OF NFH-NS ADMINISTERED VIA P.O. ROUTE ($N = 5$). ASTERISK INDICATES SIGNIFICANT DIFFERENCE BETWEEN NFH-NS AND NFH (* $P < 0.05$, $^{\#}P < 0.01$, $^{\#}P < 0.001$). BL INDICATES BASELINE

Dose response curve was constructed between dose (NFH-NS $10\text{-}30 \text{ mg kg}^{-1}$) and maximum % reversal of allodynia at corresponding dose. Maximum percent reversal was reported for highest studied dose 30 mg kg^{-1} (**Fig. 9**). Dose that produced 50 % of maximum percent reversal (ED_{50}) as calculated by curve-fitting functions in GraphPad Prism 5.01 was found 16.4 mg kg^{-1} (**Table 2**).

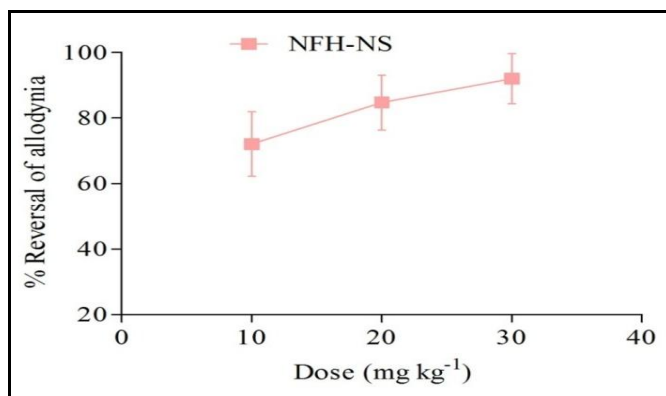


FIG. 9: MAXIMUM % REVERSAL OF ALLODYNIA PRODUCED BY NFH-NS ($10\text{-}30 \text{ MG KG}^{-1}$, P.O.) ($N = 5$)

TABLE 2: REPORTS OF NFH-NS AGAINST TACTILE ALLODYNIA IN RAT MODEL OF INCISIONAL PAIN

Compound	NFH-NS
Doses (mg kg^{-1})	10, 20, 30
Route	p.o
MED (mg kg^{-1})	10
Onset of action (h)	by 0.5
Duration of action	long
Maximum percent reversal	72, 84, 92 %
ED_{50} (mg kg^{-1})	16.4

CONCLUSION: Our findings clearly demonstrated that poly (meth) acrylates nanospheres of nefopam hydrochloride synthesized by quasi solvent diffusion technique followed fickian diffusion for drug transport with an initial 'burst release' succeeded by sustained release over 24 h. Long term and accelerated stability testing revealed stability of NFH-NS on storage at $25 \pm 2^{\circ}\text{C}/60 \pm 5\% \text{ RH}$ and $40 \pm 2^{\circ}\text{C}/75 \pm 5\% \text{ RH}$. It was investigated that maximum reversal of mechanical allodynia was achieved after p.o

administration of NFH-NS (30 mg kg⁻¹) in a rat model of post-incisional pain study. We have researched the potency and efficacy of NFH-NS in a rat model of post-incisional pain. MED and ED₅₀ of NFH-NS was found 10 mg kg⁻¹ and 16.4 mg kg⁻¹, respectively. Current investigation conclusively manifested sustained as well as dose dependent effect of NFH-NS. These findings should prove useful in the study of post-incisional pain and assessment of novel treatments.

ACKNOWLEDGEMENTS: The authors wish to thank Chitkara University for providing platform to conduct this research work. The support for providing access to Science Direct and anti-plagiarism software from department of Research, Innovation and Consultancy, Punjab Technical University, Jalandhar, is greatly acknowledged. The authors are grateful to Evonik Industries AG, Mumbai, India for providing gift sample of eudragit RL 100 and RS 100.

REFERENCES:

1. Suphiya P, Misra R, Sahoo SK: Nanoparticles: a boon to drug delivery, therapeutics, diagnostics and imaging. *Nanomedicine: Nanotechnology, Biology, and Medicine* 2012; 8:147-166.
2. Gautier JC, Grangier JL, Barbier A, Dupont P, Dussosoy D, Pastor G, Couvreur P: Biodegradable nanoparticles for subcutaneous administration of growth hormone releasing factor (hGRF). *Journal of Controlled Release* 1992; 20:67-78.
3. Gulyaev AE, Gelperina SE, Skidan IN, Antropov AS, Kivman GY, Kreuter J: Significant transport of doxorubicin into the brain with polysorbate 80-coated nanoparticles. *Pharmaceutical Research* 1999; 16:1564-1569.
4. Jiao Y, Ubrich N, Marchand-Arvier M, Vigneron C, Hoffman M: *In-vitro* and *in-vivo* evaluation of oral heparin-loaded polymeric nanoparticles in rabbits. *Circulation* 2002; 105:230-235.
5. Couvreur P: Nanoparticles in drug delivery: Past, present and future. *Advanced Drug Delivery Reviews* 2013; 65:21-23.
6. Joshi G, Kumar A, Sawant K: Enhanced bioavailability and intestinal uptake of Gemcitabine HCl loaded PLGA nanoparticles after oral delivery. *European Journal of Pharmaceutical Sciences* 2014; 60:80-89.
7. Li X, Xu Y, Chen G, Wei P, Ping Q: PLGA nanoparticles for the oral delivery of 5-Fluorouracil using high pressure homogenization-emulsification as the preparation method and *in-vitro/in-vivo* studies. *Drug Development Industrial Pharmacy* 2008; 34:107-115.
8. Sarmiento B, Ribeiro A, Veiga F, Ferreira D, Neufeld R: Oral bioavailability of insulin contained in polysaccharide nanoparticles. *Biomacromolecules* 2007; 8:3054-3060.
9. Kapfer B, Alfonsi P, Guignard B, Sessler DI, Chauvin M: Nefopam and ketamine comparably enhance postoperative analgesia. *Anesthesia & Analgesia* 2005; 100:169-174.

10. Suto T, Obata H, Tobe M, Oku H, Yokoo H, Nakazato Y, Saito S: Long-term effect of epidural injection with sustained-release lidocaine particles in a rat model of postoperative pain. *British Journal of Anaesthesia* 2012; 109:957-967.
11. Evans MS, Lysakowski C, Tramer MR: Nefopam for the prevention of postoperative pain: quantitative systematic review. *British Journal of Anaesthesia* 2008; 101:610-617.
12. Whiteside GT, Harrison J, Boulet J, Mark L, Pearson M, Gottshall S, Walker K: Pharmacological characterization of a rat model of incisional pain. *British Journal of Pharmacology* 2004; 141: 85-91.
13. Piercey MF, Schroeder LA: Spinal and supraspinal sites for morphine and nefopam analgesia in the mouse. *European Journal of Pharmacology* 1981; 74:135-140.
14. Kyung HK, Salahadin A: Rediscovery of nefopam for the treatment of neuropathic pain. *Korean Journal of Pain* 2014; 27:103-111.
15. Löscher W, Schmidt D: New Horizons in the development of antiepileptic drugs: Innovative strategies. *Epilepsy Research* 2006; 69:183-272.
16. Torres GE, Gainetdinov RR, Caron MG: Plasma membrane monoamine transporters: structure, regulation and function. *Nature Reviews Neuroscience* 2003; 4:13-25.
17. Aymard G, Warot D, Demolis P, Giudicelli JF, Lechat P, Le Guern ME, Alquier C, Diquet B: Comparative pharmacokinetics and pharmacodynamics of intravenous and oral nefopam in healthy volunteers. *Pharmacology Toxicology* 2003; 92:279-286.
18. Heel RC, Brogden RN, Pakes GE, Speight TM, Avery GS: Nefopam: a review of its pharmacological properties and therapeutic efficacy. *Drug* 1980; 19:249-267.
19. Tigerstedt I, Sipponen J, Tammisto T, Turunen M: Comparison of nefopam and pethidine in postoperative pain. *British Journal of Anaesthesia* 1977; 49:1133-1138.
20. Du MB, Aubrun F, Langlois M, Le Guern ME, Alquier C, Chauvin M, Fletcher D: Randomized prospective study of the analgesic effect of nefopam after orthopaedic surgery. *British Journal of Anaesthesia* 2003; 91:836-841.
21. Mimoz O, Incagnoli P, Josse C, Gillon MC, Kuhlman L, Mirand A, Soilleux H, Fletcher D: Analgesic efficacy and safety of nefopam vs. propacetamol following hepatic resection. *Anaesthesia* 2001; 56:520-525.
22. Brun H, Paul M, Razzouq N, Binhas M, Gibaud S, Astier A: Cyclodextrin inclusion complexes of the central analgesic drug nefopam. *Drug Development Industrial Pharmacy* 2006; 32:1123-1134.
23. Dordoni PL, Della VM, Stefanelli A, Iannace E, Paparella P, Rocca B, Accorra F: Effect of ketorolac, ketoprofen and nefopam on platelet function. *Anaesthesia* 1994; 49:1046-1049.
24. Gasser JC, Bellville JW: Respiratory effects of nefopam. *Clinical Pharmacology and Therapeutics* 1975; 18:175-179.
25. Ranjan AP, Mukerjee A, Helson L, Vishwanatha JK: Scale up, optimization and stability analysis of Curcumin C3 complex-loaded nanoparticles for cancer therapy. *Journal of Nanobiotechnology* 2012; 10:1-18.
26. Tang J, Xu N, Ji H, Liu H, Wang Z, Wu L: Eudragit nanoparticles containing genistein: formulation, development, and bioavailability assessment. *International Journal of Nanomedicine* 2011; 6:2429-2435.
27. Leroueil-Le VM, Fluckiger L, Kim YI, Hoffman M, Maincent P: Preparation and characterization of nanoparticles containing an antihypertensive agent.

- European Journal of Pharmaceutics and Biopharmaceutics 1998; 46:137-143.
28. Holm R, Müllertz A, Christensen E, Høy CE, Kristensen HG: Comparison of total oral bioavailability and the lymphatic transport of halofantrine from three different unsaturated triglycerides in lymph-cannulated conscious rats. European Journal of Pharmaceutical Sciences 2001; 14:331-337.
 29. Kathleen D, Jo V, Guy VM, Annick L: Evaluation of ciprofloxacin-loaded Eudragit RS100 or RL100/PLGA nanoparticles. International Journal of Pharmaceutics 2006; 314:72-82.
 30. Sahana B, Santra K, Basu S, Mukherjee B: Development of biodegradable polymer based tamoxifen citrate loaded nanoparticles and effect of some manufacturing process parameters on them: a physicochemical and *in-vitro* evaluation. International Journal of Nanomedicine 2010; 5:621-630.
 31. Costa P, Sousa Lobo JM: Modeling and comparison of dissolution profiles. European Journal of Pharmaceutical Sciences 2001; 13:123-133.
 32. Karasulu E, Yesim KH, Ertan G, Kirilmaz L, Guneri T: Extended release lipophilic indomethacin microspheres: formulation factors and mathematical equations fitted drug release rates. European Journal of Pharmaceutical Sciences 2003; 19:99-104.
 33. Khan KA: The concept of dissolution efficiency. Journal of Pharmacy and Pharmacology 1975; 27:48-49.
 34. Khan KA, Rhodes CT: Effect of compaction pressure on the dissolution efficiency of some direct compression systems. Pharmaceutica acta Helvetiae 1972; 47:594-607.
 35. Madaswamy SM, Si-Shen F: Pharmaceutical stability aspects of nanomedicines. Nanomedicine 2009; 4:857-860.
 36. Mulik R, Mahadik K, Paradkar A: Development of curcuminoids loaded poly (butyl) cyanoacrylates nanoparticles: physicochemical characterization and stability study. European Journal of Pharmaceutics and Biopharmaceutics 2009; 37:395-404.
 37. Brennan TJ, Vandermeulen EP, Gebhart GF: Characterization of a rat model of incisional pain. Pain 1996; 64:493-501.
 38. Stuesse SL, Crisp T, McBurney DL, Schechter JB, Lovell JA, Cruce WL: Neuropathic pain in aged rats: behavioral responses and astrocytic activation. Experimental Brain Research 2001; 137:219-227.

How to cite this article:

Singh S, Sharma N, Singla YP, Arora S and Madan J.: Poly (Meth) Acrylates Nanospheres of Centrally Acting Analgesic Drug for Postoperative Pain: *In-Vitro* and *In-Vivo* Characterization Study. Int J Pharm Sci Res 2016; 7(5): 1967-77. doi: 10.13040/IJPSR.0975-

All © 2013 are reserved by International Journal of Pharmaceutical Sciences and Research. This Journal licensed under a Creative Commons Attribution-NonCommercial-ShareAlike 3.0 Unported License.

This article can be downloaded to **ANDROID OS** based mobile. Scan QR Code using Code/Bar Scanner from your mobile. (Scanners are available on Google Playstore)